

XVII International Colloquium on Mechanical Fatigue of Metals (ICMFM17)

## 3D Morphology of Fracture Surfaces Created by Mixed-mode II+III Fatigue Loading in Metallic Materials

T. Vojtek<sup>a,b,\*</sup>, J. Pokluda<sup>a,b</sup>, A. Hohenwarter<sup>c</sup>, K. Slámečka<sup>a,b</sup>, R. Pippan<sup>d</sup>

<sup>a</sup>Faculty of Mechanical Engineering, Brno University of Technology, Technická 2, CZ–61669 Brno, Czech Republic

<sup>b</sup>Central European Institute of Technology (CEITEC), Brno University of Technology, Technická 10, CZ–61600 Brno, Czech Republic

<sup>c</sup>Department of Materials Physics, Montanuniversität Leoben, Jahnstr. 12, A-8700 Leoben, Austria

<sup>d</sup>Erich Schmid Institute of Materials Science, Austrian Academy of Sciences, Jahnstr. 12, A-8700 Leoben, Austria

---

### Abstract

This paper presents results of 3Dfractographical analysis of shear-mode fatigue cracks in ARMCO iron,  $\alpha$ -titanium, nickel and the X5CrNi18-10 steel. Observation of crack paths on a microscopic level enables us to reveal local loading modes at the crack tip under various kinds of remote loading. Experiments were done on special specimens loaded in mixed mode II+III in the near-threshold regime. Only small deviations from the plane of maximum shear stress were observed in ARMCO iron. In titanium, nickel and stainless steel the mean deviation angles were higher. In the stainless steel, the mixed-mode II+III cracks propagated in local mode I, forming a mixture of morphologies of a highly deflected mode II facets and a factory roof in mode III. Crystallographic facets were observed in all materials except for the stainless steel. The results provide a basis for an assessment of micromechanisms of mixed-mode II+III crack propagation and the related near-threshold intrinsic resistance to crack growth.

© 2014 Elsevier Ltd. Open access under [CC BY-NC-ND license](https://creativecommons.org/licenses/by-nc-nd/4.0/).

Selection and peer-review under responsibility of the Politecnico di Milano, Dipartimento di Meccanica

**Keywords:** mixed-mode II+III fatigue loading, quantitative fractography, ARMCO iron, titanium, nickel, stainless steel

---

### 1. Introduction

Observation of crack paths on a microscopic level enables us to reveal local loading modes at the crack tip under various kinds of remote loading. In the recent works [1-3], such an analysis was done for pure mode II and mode III loading which led to a proposal of relationship for intrinsic resistance to crack propagation under pure mode II near

---

\* Corresponding author. Tel.: +420-541-142-849; fax: +420-541-142-842.

E-mail address: [tomas.vojtek@ceitec.vutbr.cz](mailto:tomas.vojtek@ceitec.vutbr.cz)

threshold loading and a verification of mode-I-branching criterion. As regards mixed mode II+III loading, however, such an analysis has not yet been done except for a proposal of equivalent stress intensity factors (SIFs) [4,5]. This paper is focused on three-dimensional (3D) topography of mixed-mode II+III cracks and a comparison of the stereophoto-grammetrical data obtained from fracture surfaces of ARMCO-iron,  $\alpha$ -titanium, nickel and stainless steel. The objective is to show how each of the local modes II and III contributes to a generation of fracture surfaces. This will provide an initial viewpoint on the intrinsic resistance to crack growth under mixed mode II+III loading and an assessment of the crack growth micromechanisms (in relation to the atomistic models published in [2]).

## 2. Experiments

Experiments were done on special specimens enabling to apply simultaneously various ratios of mode II and III loading components in the near-threshold regime [2]. The specimens were made of four different materials: ARMCO iron (nearly pure polycrystalline iron), commercially pure  $\alpha$ -titanium and nickel and the stainless steel X5CrNi18-10. A special technique was employed for preparation of mode-I precracks at the beginning of the experiment. This procedure eliminating extrinsic shielding (friction and residual stress) already enabled us to perform measurements of effective values of the SIF range at the threshold for pure mode II and III loading [2,3].

Fracture surfaces were reconstructed in 3D using the stereophotogrammetry in the scanning electron microscope (SEM) [6]. Quantification of the 3D data was done by a profile analysis using cutting planes denoted by the white arrows in Fig. 1. The coordinate  $l$  passes along the line from the left to the right and the topological profiles were determined by the vertical coordinate  $z$ . These profiles were used for a measurement of angles corresponding to the average crack deviation from the plane of the maximum shear stress. The profiles running parallel to the shear direction provide angles  $\alpha$  while those of the perpendicular direction indicate angles  $\beta$ . The average deviation angles  $\gamma_{II+III} = (\alpha + \beta)/2$  are summarized in Table 1 for all investigated materials. These angles can be compared to  $\gamma_{II}$  and  $\gamma_{III}$  for respective pure modes II and III obtained as average angles related to directions parallel and perpendicular to the applied shear stress [3].

## 3. Results and discussion

The deviation angles in the ARMCO iron are relatively small (up to 20°) and the cracks propagated here in a nearly coplanar manner under shear-mode dominance. In titanium these angles were much higher compared to those in the ARMCO iron. The highest angles corresponding to nearly pure local mode I growth were measured for nickel and stainless steel. The differences can be attributed to a different number of slip systems available in crystal structures of these metals (bcc, hcp and fcc) as reported for pure mode II and III cracks in more detail in [3].

Table 1. Comparison of mean deviation angles of mode II, mode III and mixed-mode II+III cracks.

Mode	Angle	ARMCO [°]	Titanium [°]	Nickel [°]	Stainless steel [°]
II+III	$\gamma_{II+III}$	<b>15 ± 8</b>	<b>36 ± 16</b>	<b>45 ± 15</b>	<b>45 ± 15</b>
II	$\gamma_{II}$	21 ± 11	32 ± 13	45 ± 17	39 ± 5
III	$\gamma_{III}$	21 ± 13	34 ± 15	34 ± 14	32 ± 11

The average angles  $\gamma_{II}$  are nearly equal to  $\gamma_{III}$  ones in ARMCO iron and titanium, while  $\gamma_{II} > \gamma_{III}$  in nickel and stainless steel. The latter inequality corresponds to the fact that the maximum local mode I deviations can reach 70° for remote mode II cracks but only 45° for remote mode III ones. The values of  $\gamma_{II+III}$  are rather close to those of  $\gamma_{II}$  in all materials and higher than  $\gamma_{III}$  in nickel and stainless steel. These results can be useful for a quantitative interpretation of values of the intrinsic II+III threshold in terms of an appropriate equivalent SIF ranges.

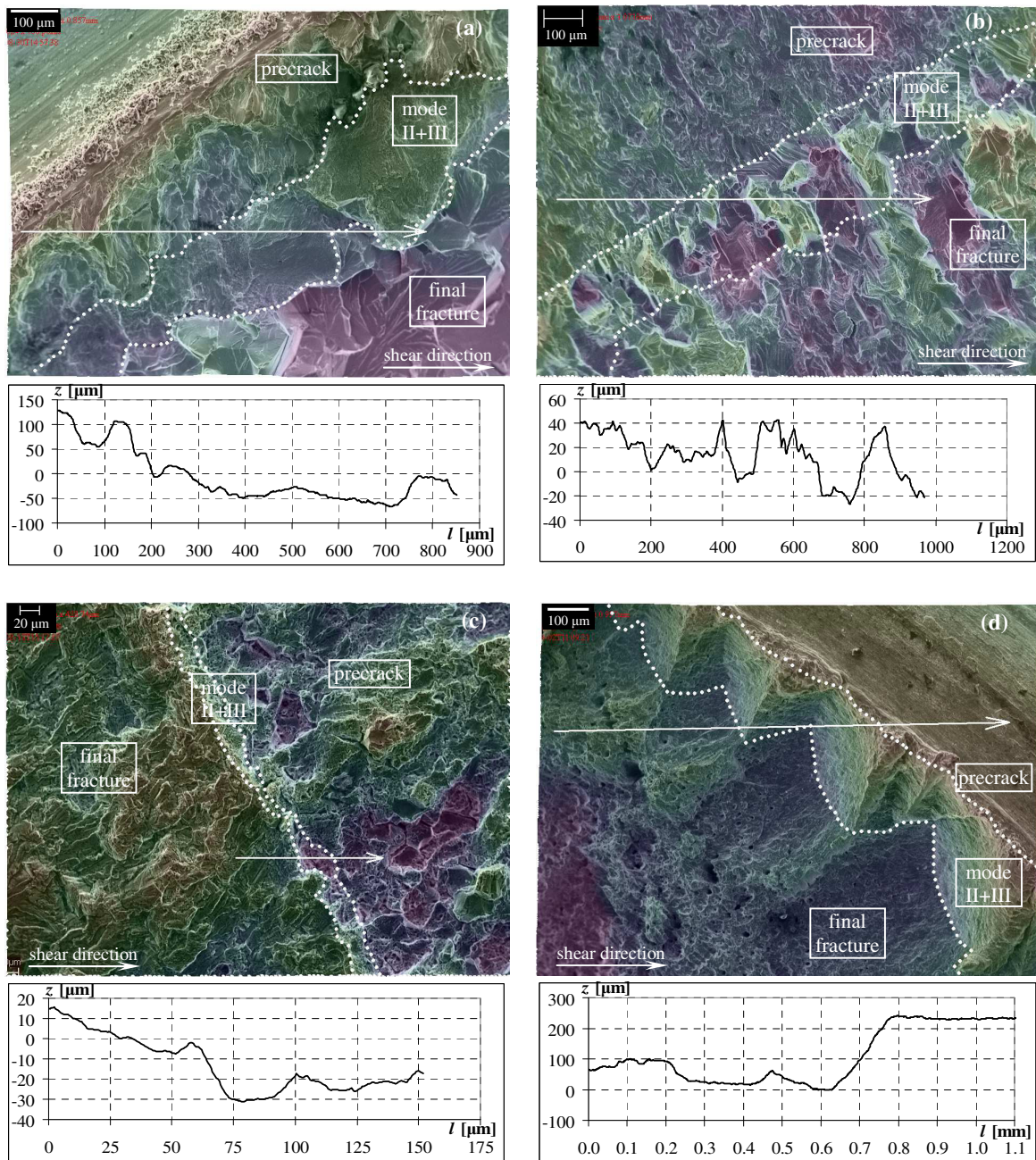


Fig. 1. Examples of fracture morphologies for remote mixed-mode II+III cracks with the height profiles corresponding to the white horizontal arrows in (a) ARMCO iron; (b) titanium; (c) nickel; (d) stainless steel.

The fracture morphologies in Fig. 1(a), (b), (c) reveal an evidence of crystallography-controlled crack propagation for ARMCO iron, titanium and nickel which was also observed for pure modes II and III. On the other hand, no crystallography influence can be detected in the stainless steel (Fig. 1(d)) where characteristic regular-shaped hills

are created during the remote mixed-mode II+III loading. They represent a transition between the high crack front deflection observed in pure remote mode II and the factory-roof morphology typical for pure remote mode III [1,2]. This is, most probably, caused by a local mode I crack growth mechanism according to the model of Deshpande et al. [7]. A qualitatively similar fracture morphology consisting of periodical fracture segments differently inclined to the macroscopic plane was observed by Hourlier and Pineau [8] in the high-strength low-alloy steel loaded in mixed mode I(cyclic)+III(static).

#### 4. Conclusions

Fracture surfaces generated by a mixed mode II+III near-threshold fatigue loading in ARMCO iron,  $\alpha$ -titanium, nickel and stainless steel were investigated using stereophotogrammetry in a SEM. This technique enabled us to reconstruct the 3D geometry of crack paths. The results revealed the following differences in fracture morphologies:

- Only small deviations from the plane of maximum shear stress were observed in ARMCO iron. In titanium, nickel and stainless steel, the height profiles were more tortuous, thus giving higher values of mean deviation angles.
- In the stainless steel, the cracks propagated in local mode I by forming a morphological mixture of highly deflected cracks typical for a pure remote mode II and a factory roof morphology characteristic for remote mode III.
- Influence of crystallography was observed in all materials except for the stainless steel.

Crack closure effects were eliminated at the beginning of the experiments due to a special technique for precrack preparation and, therefore, the obtained results provide a useful basis for an assessment of micromechanisms of mixed-mode II+III crack propagation and a quantitative interpretation of values of the intrinsic II+III threshold in these materials.

#### Acknowledgements

This work was supported by the Czech Science Foundation in the frame of the project No. P107/12/0800 and by the European Regional Development Fund (CEITEC CZ.1.05/1.1.00/02.0068).

#### References

- [1] T. Vojtek, J. Pokluda, A. Hohenwarter, R. Pippan, Three-dimensional Morphology of Fracture Surfaces Generated by Modes II and III Fatigue Loading in Ferrite and Austenite, *Engineering Fracture Mechanics* 108 (2013), 285–293.
- [2] T. Vojtek, R. Pippan, A. Hohenwarter, L. Holáň, J. Pokluda, Near-threshold Propagation of Mode II and Mode III Fatigue Cracks in Ferrite and Austenite, *Acta Materialia* 61 (2013), 4625–4635.
- [3] J. Pokluda, R. Pippan, T. Vojtek, A. Hohenwarter, Near-threshold Behaviour of Shear-mode Fatigue Cracks in Metallic Materials, *Fatigue & Fracture of Engineering Materials & Structures* 37 (2014), 232–254.
- [4] V. Doquet, Q.H. Bui, G. Bertolino, E. Merhy, L. Alvez, 3D shear-mode fatigue crack growth in maraging steel and Ti-6Al-4V, *International Journal of Fracture* 165 (2010), 61–76.
- [5] T. Vojtek, J. Pokluda, P. Šandera, J. Horníková, K. Slámečka, A. Hohenwarter, R. Pippan, Near-threshold Fatigue Crack Propagation under Mixed-mode II+III in ARMCO Iron, in: R. Goldstein (Ed.) *Fracture Mechanics for Durability, Reliability and Safety (ECF19)*, Scientific Centre of the Russian Academy of Sciences, Kazan, 2012, p. 188.
- [6] J. Stampfl, S. Scherer, M. Gruber, O. Kolednik, Reconstruction of surface topographies by scanning electronmicroscopy for application in fracture research, *Appl. Phys. A* 63 (1996), 341–346.
- [7] V.S. Deshpande, A. Needleman, E. Van der Giessen, A discrete dislocation analysis of near-threshold fatigue crack growth, *Acta Materialia* 49 (2001), 3189–3203.
- [8] F. Hourlier, A. Pineau, Propagation of Fatigue Cracks under Polymodal Loading, *Fatigue & Fracture of Engineering Materials & Structures* 5 (1982), 287–302.